

Agricultural Greenhouses: climate optimization, simulation by TRNSYS for Predicting Crop Yield and Energy Consumption

Douja Sellami^{#1}, Sami Kooli^{#2}

[#] *Laboratory of Thermal Processes; Research and Technology Center of Energy, Borj Cedria, Tunisia*

Email 1 - Sellami.douja@gmail.com

Abstract

This paper describes a method of modelling the performance of greenhouses. The method was developed to assist in the design of low energy protected cropping structures to be used in the inland climates of Tunisia.

To facilitate the modelling procedure, a greenhouse is considered to be composed of a number of separate but interactive components. These are the cover, floor, growing medium, air space and crop. A particular feature is the use of a tomato crop model which responds to photosynthetically active radiation, leaf temperature and CO₂ level. Integrating biological parameters into simulation can improve understanding of the complex interactions between climate, plants, and overall greenhouse performance.

Field tests were conducted to test diurnal variations of temperature, relative humidity, and solar radiation and to analyze the microclimate characteristics in a ventilated chapel-shaped greenhouse. Design criteria were that the greenhouses shouldn't use any amount of conventional energy for heating.

This study provides a reference for further research to reduce energy consumption and achieve a favorable greenhouse microclimate, leading to higher product quality, improved yield and shorter cultivation time in chapel-shaped greenhouses.

The paper presents details of the mathematical models of each component and lists the assumptions used with each. The simulated performance of the greenhouse in winter is presented and an analysis of the simulated crop yields, energy flows and temperatures indicates that the model is simulating the expected trends in greenhouses.

Keywords: TRNSYS; chapel-shaped style solar greenhouse; energy; solar radiation, evapotranspiration

Symbols Definition Unit

C_i : Thermal capacity of indoor air J.Kg⁻¹.K⁻¹

V : Mass air flow (by ventilation, infiltration) Kg h⁻¹

ρ_{air} : Air density Kg.m⁻³

h : Convective heat transfer coefficient W.m⁻².K⁻¹

$\epsilon_{s,o}$: Long wavelength emissivity of the exterior surface ($\epsilon = 0.9$ for walls; value read from the window library)

σ : Stephan-Boltzmann constant $\text{w.m}^{-2} \text{K}^4$

f_{sky} : Fraction of the sky seen from the exterior surface (we take the value 0.5 for vertical surfaces and value 1 for horizontal surfaces)

L : Specific latent heat of vaporization of water J Kg^{-1}

$W_{g,i}$: Water vapor flow evaporated by the plant cover Kg s^{-1}

A_p : Leaf surface m^2

W_p^* : Saturating specific humidity of air at temperature of the plant $\text{Kg H}_2\text{O/Kg of dry air}$

W_a : Ambient air humidity

r_{ap} : Total resistance to water transfer s m^{-1}

r_a : Aerodynamic resistance s m^{-1}

r_p : Stomatal resistance s m^{-1}

Δt : Simulation time interval s

m : Air flow Kg s^{-1}

K : Relative to user-defined time base

$q_{s,i}$: Heat flow by conduction towards the internal wall surface W

N : Air renewal rate h^{-1}

max : Maximum

min: Minimum

LAI: Leaf area index

λ_s : Conductivity $\text{W m}^{-1} \text{K}^{-1}$

ρ_s : Density Kg m^{-3}

G : solar radiation W m^{-2}

U : Wind speed ms^{-1}

RH : Relative humidity $\%$

T : Temperature $^{\circ}\text{C}$

NT: Night temperature $^{\circ}\text{C}$

DT: Daytime temperature $^{\circ}\text{C}$

T_{ai} : Indoor air temperature $^{\circ}\text{C}$

T_p Plant temperature $^{\circ}\text{C}$

ET :Evapotranspiration of the plant $\text{mg.m}^{-2}\text{s}^{-1}$

Q : Heat Heating requirement MJ

I. Introduction:

Climate change is one of the most challenging problems of the modern world. Regarding climate change issues which coincided with rising of several environmental threats the challenge to sustainable development is becoming more and more important worldwide. The pressure put on the environment through unsustainable conducts by modern agricultural techniques (Das, 2014) will distinctly possible exacerbate because of global population growth and climate change, which is in need of more efficient agricultural systems in terms of time and quantity. Rapid population growth and the desire for a better quality of life are among the factors leading to increased demand for many products. This leads to economy's growth but have a drastic impact on environment resource resulting from this excessive utilization as mentioned by (Nathaniel, 2020) who proved that along with increasing human consumption, climate change is increasing the vulnerability of societies and intensifying the scarcity of ecological resources. Moreover, worldwide, researchers contend that climate change and environmental problems are due to inadequate natural resource management. According to I. Khan et al. (2022), especially in the wake of the pandemic a surging demand for production and industrialization exacerbated resource depletion for energy production which deeply concerns among global economists. However, in the later stages of economic development, along with improving the quality of human life, nations think about the degrading environment and seek energy-efficient and environmentally friendly resources (Zafar et al., 2019). As different economies address issues of climate change and energy security in their roadmaps, previous research paves the way for energy efficiency (Zhang et al., 2022).

Therefore, energy efficiency improvements used to be increased speed and seriously (Sinha et al., 2020, Sinha et al., 2017). Alongside energy efficiency, renewable energies are the main elements enabling global energy transformations. Moreover, in the last stages of economic development, with the improvement of the quality of human life, nations have finally thought about the deterioration of natural environmental resources and are looking for energy-saving and environmentally friendly resources environment (Zafar et al., 2019). Natural resources, once seen primarily as tools of production and industrialization, have become symbols of power, domination, and diplomatic leverage for nations blessed with such resources. The critical input in a production process is energy, but the literature only focuses on overall production efficiency rather than energy efficiency until Hu and Wang (2006), who propose the idea of total-factor energy efficiency.

Among the disaggregated efficiencies proposed by Hu and Wang (2006), there is energy efficiency. Luthra et al. (2022) study the links between the circular economy, the valorization of natural resources, the efficiency of material resources and energy efficiency. Especially emerging economies which benefit from their practical observations and policy recommendations.

Energy efficiency is heralded as a crucial aspect of sustainable development, representing the utilization of the same amount of energy while minimizing wasteful practices to reduce consumption through technological advances. According to Siano (2014), improving energy efficiency plays a crucial role in reducing energy consumption. Energy environmental sustainability embodies the transformation of energy system of country to extenuate potential climate change harms and environmental damage. But there is a contradiction between higher demand of fossil energy and exacerbating climate change (Pan et al., 2023; Mao et al., 2023). To relieve the hard disagreement, the move to clean energy focusing low environmental load is crucial (Yang and Wang, 2022; Lin and Li, 2022).

The availability of natural resources and its accessibility, enclosing renewable energy, fossil fuels, and biomass, play a key role in enhancing economic sustainability.

Forest resources, which provide biomass energy are an essential component of energy efficiency, but mineral resources, including renewable energy sources, facilitate the development of supporting technologies, which are part integral to realize sustainable energy efficiency.

According to (Guo et al., 2020), the optimal design of solar greenhouses can reduce environmental impact, which can increase land use efficiency and reduce water use and pesticides at the same time.

As the world's largest energy producer and carbon emitter, the total energy consumption of China has maintained a substantial growth (Liu et al., 2022).

Currently, agricultural greenhouses are among the most energy-intensive sectors. As a result, the cost and environmental sustainability of greenhouse production are largely driven by the demand for fuels and electricity to meet the heat needs of greenhouses, especially in applications located in cold climates. It is the well-being of crops which results in high control of the indoor microclimate which consumes a lot of energy. Thus, to increase plant growth, specific values of indoor air temperature, relative humidity and CO₂ concentration are necessary (Yohannes and Fath, 2013).

Water absorption and transpiration play a crucial role in the development of horticultural crops while ensuring the transport of nutrients to plant organs. There is also an interaction between moisture and photosynthesis and dry matter production, affecting either leaf surface development or stomatal conductance. Thus, integrating biological parameters into simulation can improve understanding of the complex interactions between climate, plants, and overall greenhouse performance. Tiwari (1984) examined the influence of different parameters and also studied the effects of the temperature of a mobile insulation system on the air and plants in the greenhouse.

TRNSYS is a program with discretization functionalities (Yu et al., 2016). TRANSSOLAR Energietechnik (Henshaw, 2016) calls the thermal point of TRNSYS an "air node". Simulating multiple aerial node zones is a refined modeling capability. TRNSYS, a software developed by the University of Wisconsin Solar Energy Laboratory, stands for Transient System Simulation and is among the most popular software for greenhouse simulation (Semple et al., 2017). The major advantage of using TRNSYS is that its prediction is more precise. It also allows the simulation of several thermal nodes.

Evapotranspiration from crops in a greenhouse has been proved to affect the energy balance of the greenhouse (Ahamed et al., 2018) as well as the temperature difference between the crop and the immediate ambient air (Attar et al., 2013). Therefore, researchers thought about integrating different crop models into building energy simulation (BES) models as energy gain or loss.

Modeling greenhouse thermal environments using construction software is relatively complicated compared to traditional buildings owing to the dynamic nature of plants through photosynthesis and transpiration. Furthermore, environmental control systems as well as suggested operating practices in greenhouses are very diverse to maintain optimal internal microclimates for several plants which includes temperature, relative humidity, CO₂ and light. Previous thermal modeling of the greenhouse environment using building simulation software has not considered the plants in the greenhouse (Ha et al., 2015; Henshaw, 2016; Deiana et al., 2014) or assumed that evapotranspiration is constant in greenhouses (Vadiee et al., 2013,

Semple et al., 2017; Semple et al., 2016). These assumptions likely lead to significant errors in the simulation since the sources of heat and humidity in productive greenhouses are dynamic and extremely dependent on plant conditions and solar radiation (Shamim et al., 2020).

In this context, our paper denotes energy efficiency in an agricultural greenhouse. This study examines the biological parameters linked to the well-being of plants through a simulation using the TRNSYS software. The document presents a simulated performances of a thermally insulated agricultural greenhouse grown with plants. The plant cover is not a passive element within the greenhouse; it participates in the exchanges of energy (gain on the plant cover) and mass (gain on the air inside the greenhouse). It can therefore modify the energy and water vapor balances and consequently the indoor climate (temperature and humidity of the indoor air). Different climatic and biological parameters are presented and an analysis of simulated crop yields, energy flow and temperatures indicate that the model simulates expected trends in greenhouses

In this work, we are interested in characterizing the functioning of the complex system that constitutes a passive solar greenhouse with its different compartments (floor, cover, culture, wall, interior and exterior environments), by developing a model on TRNSYS which makes it possible to reproduce the essential properties, mechanisms and interactions between the different compartments and to approach quantitatively and qualitatively the analysis of its thermo-energetic behavior.

II. Material and Method

TRNSYS is considered for this study because it is a widely used. TRNSYS is a simulation tool which has a wide range of models which cover both the building and the technical and regulation equipment. TRNSYS also has a mechanism for the user to add their own component models. This is what has made it popular with the research community and design offices specializing in the search for innovative solutions, particularly in terms of the integration of technical equipment (multi-source/multi-energy system) and renewable energies. TRNSYS therefore constitutes a dynamic building simulation platform.

For the greenhouse, such a research platform in the field of renewable energies and climate control in the greenhouse constitutes a valuable tool allowing us to move towards optimization of energy consumption while improving the quality and quantity of production. To date, such a platform has not yet been developed. The objective of this work is to study the possibilities of modeling the greenhouse on TRNSYS in order to take advantage of this dynamic simulation environment.

1. Description of the chapel greenhouse with vegetation modeling using TRNSYS

The TRNSYS simulation model for the chapel greenhouse with vegetation consists of many components, including weather data, solar radiation, and multizone building components, as well as control systems.

Thermal transfers within the greenhouse are treated using the “Type56” component from TRNSYS, designed for buildings. Type 56 is of particular importance because it is an open component of TRNSYS, which allows multiple possibilities. Type 56 is a “non-geometric” balance model, which assigns a node to each zone. Several heat flows come into play in balancing the thermal load of a building. These flows depend on the architecture of the room (wall, floor, window, etc.), weather conditions (solar radiation, ambient air temperature, wind speed, atmospheric pressure, humidity, etc.), occupants and auxiliary equipment.

The greenhouse presents a thermal behavior quite different from residential buildings, due to its particular characteristics:

- A lightweight structure supporting a transparent envelope with low inertia which transmits a large part of solar radiation.
- A culture which captures the majority of this radiation and transforms it largely into latent heat of vaporization (plant transpiration) and sensible heat. It therefore participates in energy and mass exchanges.
- A ground which absorbs incident radiation and transforms part of it into latent heat.
- The ground constitutes most of the thermal mass of the greenhouse, unlike buildings where the walls and roof are the predominant storage elements.
- The greenhouse is characterized by the importance of heat transfer phenomena by radiation, by conduction, by convection and by leakage.

A schematic layout of the developed model is presented in Fig 1.

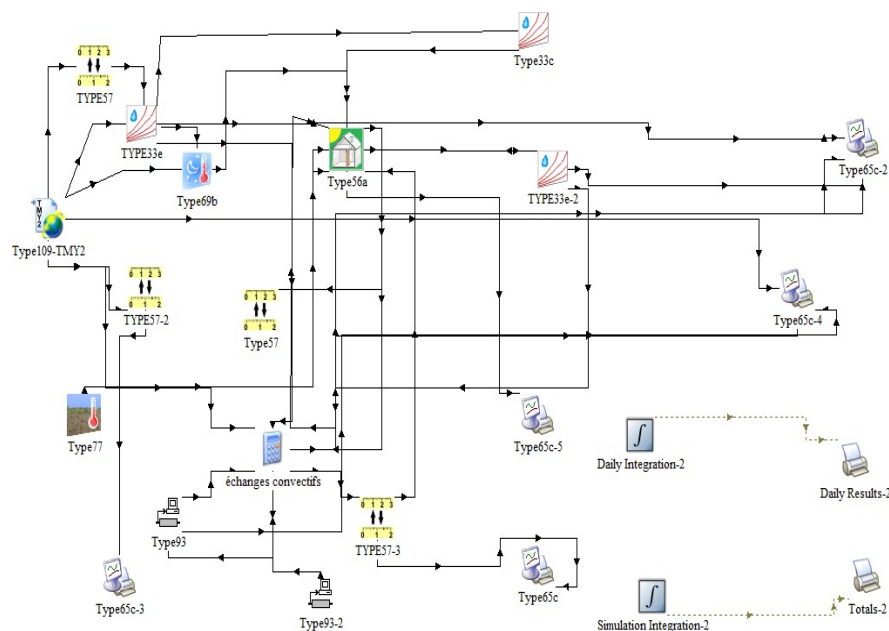


Fig. 1: TRNSYS graphical interface containing the simulation diagram /Components of the TRNSYS heating simulation model for a chapel greenhouse with vegetation.

2. Greenhouse building parameters

The greenhouse that we propose to study is a solar greenhouse with a sloping roof. Its north face is made up of a wall of length $L = 12.5$ m; its height is $h = 3$ m. Its design has an effect on the inner microclimate, in particular the south wall strongly influences the use of solar energy.

The greenhouse is represented as a system made up of four distinct parts: the cover separating the interior from the exterior, the interior air, the vegetation and the soil. These environments are the site of heat and mass exchanges summarized in Fig 2.

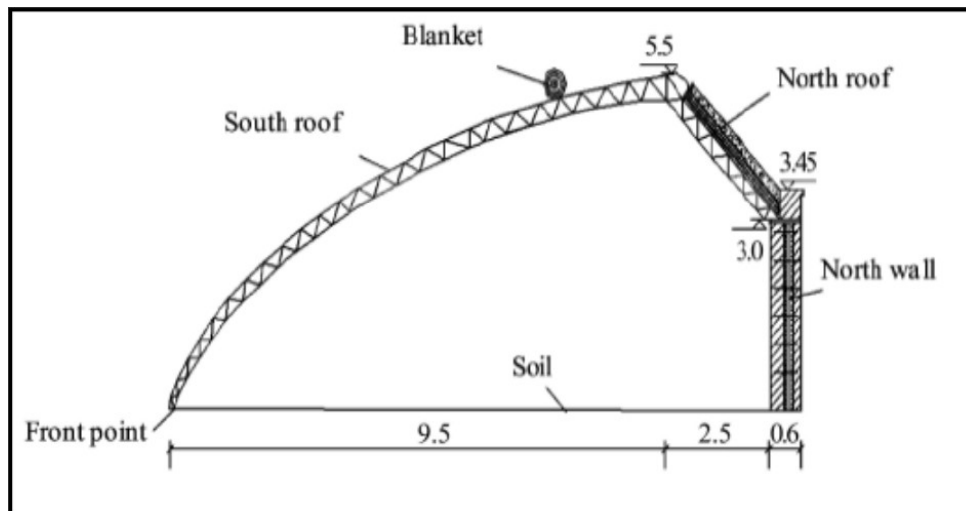


Fig 2: Side view of a typical solar greenhouse with dimensions in meters

The south roof is a thin transparent surface made of plexiglass which transmits solar rays into the interior of the greenhouse during the day.

The north wall is a sandwich panel. The height, thickness and composition of the north wall all affect the amount of solar energy stored in the wall during the day.

At night, an automatic shutter is removed over the south roof to keep the heat inside. The shape and angle of the south roof influence the reflection and transmission of solar insolation and the amount of solar energy absorbed inside the greenhouse. Thus, they represent the most important cross-sectional parameters.

The main function of the south wall apart from the load bearing is its ability to absorb solar energy during the day and release heat to the inside during the night to conserve the energy inside the greenhouse.

The north roof is a non-transparent roof made of light materials, such as sandwich panels knowing that a longer north roof improves the energy conservation when the span and height are kept constant (Tong et al, 2013). However, a longer north roof also increases the shading below the north roof when the sun is high in the sky. Practically, the length of the north roof horizontal projection is used instead of the length of the north roof during the design and construction. When the length of the north roof horizontal projection is kept constant, changes in the north roof angle change the amount of solar insolation intercepted by the north roof, the north wall and the soil surface.

The energy analysis presented in this section is primarily based on the first law of thermodynamics. The theoretical model used for the study of the greenhouse consists of using a thermal energy balance during the plant growth phases.

Table 1: Characteristics of the sandwich panel wall used in modeling of the solar greenhouse using TRNSYS.

Kind	Layers	Thickness (m)	Resistance (hm ² K/KJ)	Conductivity (J/hmK)	Capacity (KJ/KgK)	Density (Kg/m ³)
Sandwich Panel	Galvanized sheet	0.007	1.21	52	0.1	0.1
	Poly-Exp	0.040		0.141	1.38	25
	Polyurethane	0.100		0.108	0.837	35

a. The indoor air

The indoor air, treated in a single homogeneous block (zone i), is characterized by its temperature (T_i) and its specific humidity (w_i) It is the seat of the following exchanges:

-The exchange of sensible heat, inside the greenhouse, by convection, with the roof, the plant cover and the ground represented by $Q_{surf,i}$;

-Sensible heat exchanges by air infiltration, represented by $Q_{inf,i}$;

-Sensible heat exchanges by ventilation, represented by $Q_{vent,i}$;

the internal convective exchanges represented by. $Q_{g,c,i}$. This heat flow is planned by TRNSYS to take into account convective exchanges due to occupants, equipment, lighting, radiators, etc....

The energy balance of indoor air is written:

$$C_i \frac{dT_i}{dt} = Q_{surf,i} + Q_{inf,i} + Q_{vent,i} + Q_{g,c,i} \quad (1)$$

with

$$Q_{inf,i} = \rho_{air} \cdot C_p \cdot V_{inf} \cdot (T_v - T_i) \quad (2)$$

$$Q_{vent,i} = \rho_{air} \cdot C_p \cdot V_{vent} \cdot (T_v - T_i) \quad (3)$$

$$Q_{g,c,i} = 0 \quad (4)$$

Where V: represents the mass flow of air (by ventilation, infiltration)

T_v : the temperature of the ventilated air

T_i : the temperature of the air node of the zone

C_p : specific heat capacity

ρ_{air} : air density

b. The cover

The roof of the greenhouse is treated in six homogeneous blocks (six exterior walls; North, South, East, west, and north and south roof) The architectural design of the roofing was chosen

so that the south wall and the south roof receive the maximum visible radiation during the winter and the minimum during the spring and summer.

External faces of the cover are the site of the following exchanges:

*heat exchanges by conduction, represented by $q_{s, o}$;

*long-wave radiative exchanges with the outside world represented by $q_{r,s,o}$;

*radiative exchanges of short wavelengths represented by $S_{s, o}$;

*exchanges of sensible heat, by convection, with the outside air represented by $q_{c,s,o}$;

*The combined heat flow exchanged by convection and radiation $q_{comb,s,0}$ with external surfaces is written as:

$$q_{comb,s,0} = q_{c,s,o} + q_{r,s,o} \quad (5)$$

With:

$$q_{c, s, o} = h_{conv, s, o} (T_{a, s} - T_{s, o}) \quad (6)$$

$$q_{r, s, o} = \sigma s_{s, o} (T_{s, o}^4 - T_{fsky}^4) \quad (7)$$

$$T_{fsky} = (1-f_{sky}) T_{a, s} + f_{sky} T_{sky} \quad (8)$$

where

$h_{conv, s, o}$: Coefficient of heat transfer by convection at the exterior surface.

$T_{a,s}$:: outside air temperature

$T_{s,o}$: temperature of the external surface of the wall

$s_{s,o}$: long-wavelength emissivity of the exterior surface ($\varepsilon = 0.9$ for walls; value

read from the windows library)

σ : Stephan-Boltzmann constant

$T_{f,sky}$: fictitious temperature of the sky

f_{sky} : Fraction of the sky seen by the exterior surface (we take the value 0.5 for vertical surfaces and value 1 for horizontal surfaces)

T_{sky} : sky temperature

The energy balance at the level of the external surfaces of the roof is written:

$$q_{s, o} = q_{comb, s, o} + S_{s, o} \quad (9)$$

The internal faces of the cover are:

- heat exchanges by conduction, represented by $q_{s, i}$;

- long-wave radiative exchanges with the plant cover and the soil represented by $q_{r,s,i}$;

- the radiative exchanges of short wavelengths represented by $S_{s, i}$;

- the exchanges of sensible heat, by convection, with the indoor air represented by $q_{c,s,i}$;

- supplemental internal exchanges, represented by q_{supl} . This additional heat flow is provided by TRNSYS to model floor heating and roof cooling panels, etc....

The combined heat flow exchanged by convection and radiation with the internal surface is written:

$$q_{\text{comb},s,i} = q_{c,s,i} + q_{r,s,i} \quad (10)$$

The energy balance at the level of the internal surfaces is then written:

$$q_{s,i} = q_{\text{comb},s,i} + S_{s,i} + q_{\text{supl}} \quad (11)$$

With

$$q_{\text{supl}} = 0$$

c. The plant cover

Shamim et al. (2020) announced that the heat capacity of the zone must be simulated in the presence of plants. However, the crop density (weight of plant mass per unit of floor space) in the greenhouse can be significantly different from the planting time until maturity. Therefore, since it is impossible to change the heat capacity throughout the year, Semple et al. (2017) used a constant crop density of 6.0 kg m^{-2} and assumed that the thermal properties of crops are similar to those of water.

The plant cover, treated in a single homogeneous block, can be considered as an internal wall, with opaque surfaces. It is assumed that the thermal inertia of the plant cover is negligible. The state variable that characterizes the plant cover is the temperature of the leaves (T_p). The plant cover is the seat of the following exchanges:

- heat exchanges through the plant cover by conduction, represented by $q_{s,i}$;
- long-wave radiative exchanges with the cover and the ground represented by $q_{r,s,i}$;
- the radiative exchanges of short wavelengths represented by $S_{s,i}$;
- the exchanges of sensible heat, by convection, with the indoor air represented by $q_{c,s,i}$;
- latent heat exchanges by evapotranspiration, represented by q_{supl} This additional heat flow is provided by TRNSYS to model the heating of the floor and the cooling panels on the roof, etc.... We use this flow to model the evapotranspiration of plants.

The energy balance at the plant cover level is then written:

$$q_{s,i} = q_{\text{comb},s,i} + S_{s,i} + q_{\text{supl}}$$

The latent heat flows exchanged by convection between the indoor air and the plant cover are written as:

$$q_{\text{supl}} = LW_{g,i} \quad (12)$$

where

L: the specific latent heat of vaporization of water (J kg^{-1}),

$W_{g,i}$:the flow of water vapor evaporated by the plant cover (kg s^{-1})

The transpiration flow of the plant cover is given by the following equation (Penman, 1948) [68]:

$$W_{g,i} = A_p \rho_a \left(\frac{W_a - W_p^*}{r_{ap}} \right) \quad (13)$$

Where

A_p : leaf surface

W_p^* : the specific saturating humidity of the air at the temperature of the plant

W_a : humidity of the ambient air

r_{ap} is the total resistance to water transfer

r_{ap} is the sum of the aerodynamic resistance: $r_a = \frac{\rho_a C_{p_a}}{h_{ap}}$, and a stomatal resistance, r_p .

For modeling stomatal resistance, we use the multiplicative model of JARVIS (1976) [69], which was subsequently taken up by Stanghellini (1987) and Stanghellini and de Jong (1995). This model is of the form:

$$r_p = r_{\min} f_1(I_s) f_2(T_p) f_3(W_p^* - W_a) \quad (14)$$

Where r_{\min} is the minimum stomatal resistance obtained under optimal climatic conditions (82 sm^{-1}) on a tomato cover; f_1 , f_2 and f_3 are three mathematical functions which represent the evolution of stomatal resistance as a function of the climatic variables considered and I_s is the average of the short wavelength radiation arriving at the vegetation level.

$$r_p = r_{\min} \left[\frac{I_s + 4,30}{I_s + 0,54} \right] \left[\frac{e^{0,3T_p} + 258}{e^{0,3T_p} + 27} \right] \left[4 \cdot 10^{-3} + e^{-0,73 \left(\frac{W_p^* - W_a}{W_p^* - W_a} \right)} \right]^{\frac{1}{4}} \quad (15)$$

d. The soil

The ground, treated as a single homogeneous block, can be considered as a wall, with opaque surfaces, with known boundary conditions. The state variable which characterizes the soil is the temperature of the air-soil interface, T_s .

The energy balance at ground level is written:

$$q_{s,i} = q_{\text{comb},s,i} + S_{s,i} + q_{\text{supl}}$$

With $q_{\text{supl}} = 0$;

The soil boundary condition is the deep soil temperature. It is determined by Type 77.

This subroutine calculates the ground temperature at a given depth using the formula from Kasuda (1965):

$$T = T_{\text{mean}} - T_{\text{amp}} \cdot \exp \left[-\text{depth} \cdot \left(\frac{\pi}{365\alpha} \right)^{0.5} \right] \cdot \cos \left\{ \frac{2\pi}{365} \cdot [t_{\text{now}} - t_{\text{shift}} - \frac{\text{depth}}{2} \cdot \left(\frac{365}{\pi\alpha} \right)^{0.5}] \right\}$$

T (°C): temperature

T_{mean} (°C): annual average ground surface temperature (mean air temperature).

T_{amp} (°C): amplitude of the ground temperature (maximum air temperature minus the minimum air temperature).

depth (m): depth below the ground surface (taken in our example at 0.62 m)

α (m²/day): the thermal diffusivity of the soil

t_{now} (day): current day of the year

t_{shift} (day): day of the year corresponding to the minimum surface temperature

T_{initial} (°C): initial temperature

3. Balance sheet equations

a. Thermal balance (unheated greenhouse):

The energy balance of indoor air is written:

$$C_i \frac{dT_i}{dt} = Q_i$$

With

$$Q_i = Q_{\text{surf},i} + Q_{\text{inf},i} + Q_{\text{vent},i} + Q_{\text{g,c},i} \quad (16)$$

where $Q_{\text{surf},i}$ is the convective gain from surfaces; $Q_{\text{inf},i}$ is the infiltration gain; $Q_{\text{ven},i}$ is the ventilation gain; $Q_{\text{cg},i}$ is the internal convective gain (people, equipment, illumination, radiators, etc.);

b. Water balance

The indoor air (under the greenhouse) is also the site of water vapor exchanges by condensation on the internal faces of the cover, by evapotranspiration from the plants, by evaporation on the surface of the soil and by air renewal. Neglecting the effect of condensation on the internal surface of the roof and by evaporation on the surface of the ground, the mass balance of the indoor air is written:

$$M_{\text{eff},i} (d\omega_i)/dt = m_{\text{infl}} (\omega_a - \omega_i) + m_{\text{v}} (\omega_v - \omega_i) + W_{\text{g},i}$$

With

$$M_{\text{eff},i} = \text{Ratio } M_{\text{air},i}$$

Or

$M_{\text{eff},i}$: effective water capacity of indoor air

$M_{\text{air},i}$: indoor air mass

Ratio: multiplication factor, between 1 and 10

m_{infl} : air flow due to leaks (kg s⁻¹)

m_{v} : air flow due to forced ventilation (kg s⁻¹)

ω_a : specific humidity of ambient (outdoor) air (kg of water/kg of dry air)

ω_i : specific humidity of indoor air (kg of water/kg of dry air)

ω_v : specific humidity of the air exchanged by ventilation (kg of water/kg of dry air)

$W_{g,i}$: internal humidity gains. We use this additional (additional) mass flux, predicted by TRNSYS, to take into account the effect of the flow of water vapor evaporated by the plant cover on the indoor climate.

Type 56 calculates the water balance, in parallel with the sensible energy balance. In order to simplify the solution of the simultaneous set of equations, the value of ω at the end of the previous time step is used in the expression above.

Evapotranspiration (ET) of plants in greenhouses plays a crucial role in the energy balance of greenhouse microclimates. Knowing that evaporation and transpiration occur simultaneously and it is very difficult to isolate these two processes; therefore, it is a combined phenomenon which is evapotranspiration. The moisture produced by evapotranspiration depends on various factors, including solar radiation, vapor pressure deficit, air velocity, plant types as well as cross-cultural practices in greenhouses. Katsoulas and Kittas (2011) showed that among these factors, solar radiation is highly correlated with moisture production in greenhouses, and daytime crop transpiration is high relative to growth medium evaporation. However, it is almost impossible to model the real transient scenario of humidity production in greenhouses using TRNSYS. So, evapotranspiration in greenhouses is modeled by adhering an internal humidity gain with a planning type manager.

III. Results:

1. Outdoor climate

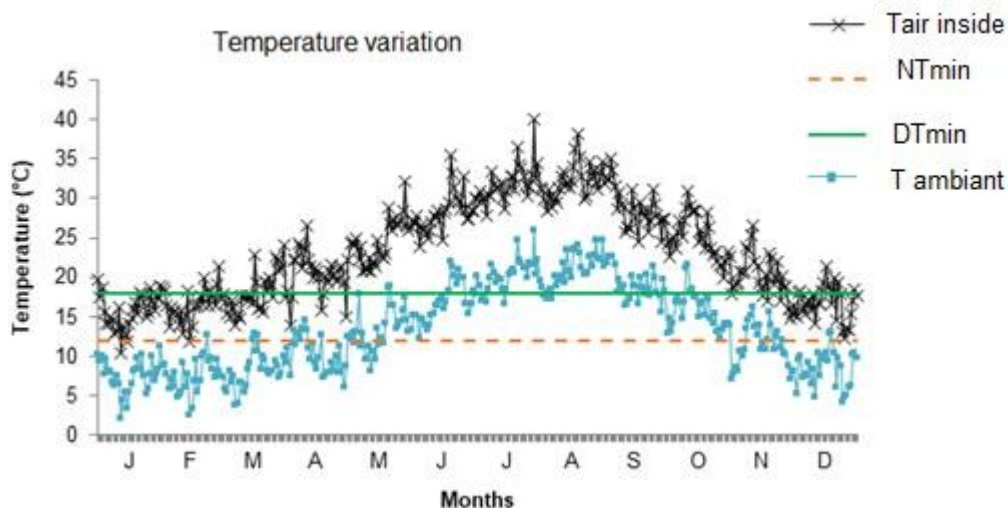


Fig 3: Outdoor air temperature variation curves and permissible temperature limits for tomato growing depending on the months of the year.

We represent in figure 3 the ambient temperature outside, the minimum nighttime ($NT_{min}=12^{\circ}\text{C}$ for tomatoes) and daytime ($DT_{min}=18^{\circ}\text{C}$) temperatures required by the plant, depending on the months of the year. We note that a temperature difference between day and night ($DT_{min} - NT_{min}$) of about 6°C is essential to ensure good initiation and flowers formation. We note that during the months of May, June, July, August, September and October, the temperatures are favorable for good growth of the plant.

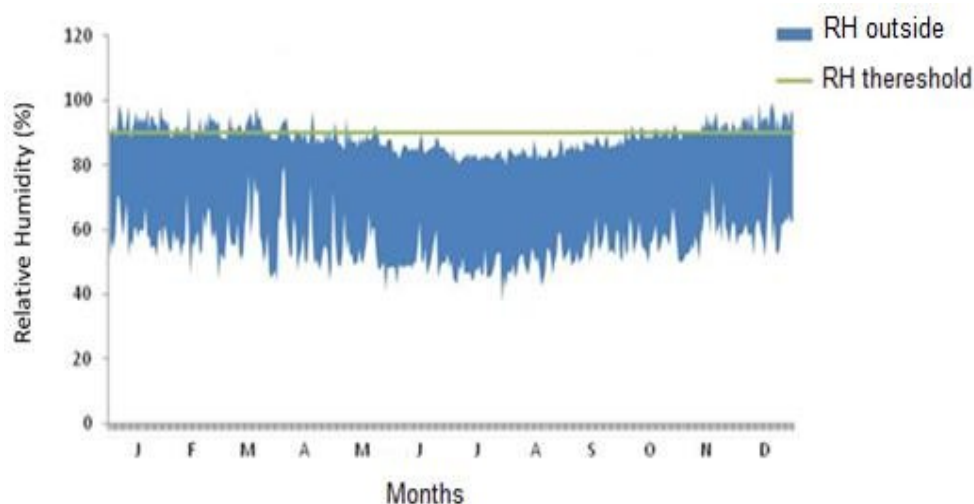


Fig 4: Relative humidity variation curves depending on the months of the year.

Figure 4 shows the curves of outside relative humidity as a function of the months of the year as well as the maximum admissible humidity for the plant. We note that during the same period from May to October, the relative humidity of the outside air (less than 90%) is favorable for good growth of the plant.

Large spatial differences of air temperature and other micro-meteorological parameters would affect the physiological responses of numerous plants including the transpiration process and thermal time of phenological responses in the flowering and maturity stage (Savage, 2014).

In figure 5, we represent the wind speed as a function of the months of the year. We found that the wind intensity is uniformly distributed throughout the year and that the wind speed varies on average between 2 m/s (minimum average) and 8 m/s (maximum average).

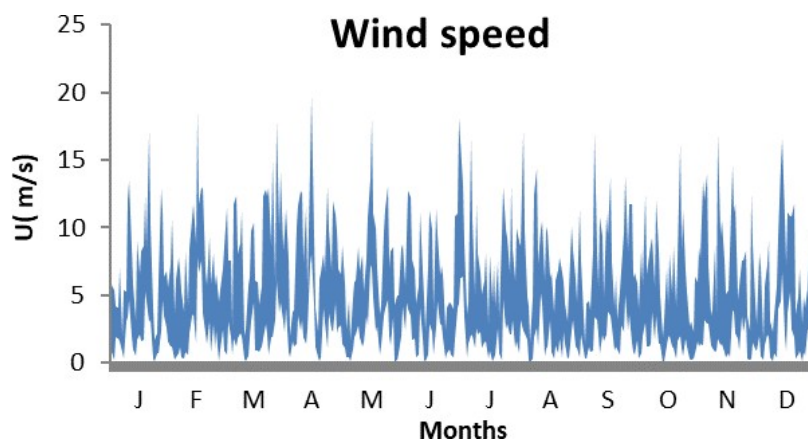


Fig 5: Wind speed variation curves depending on the months of the year.

Figure 6 represents the direct solar radiation (daytime maximums) reaching the four main surfaces of the greenhouse (north and south wall, north and south roof) as a function month of the year. We found that the south roof and south wall receive the greatest amount of solar

radiation. Solar radiation enters the greenhouse through the north wall and the north roof only during the warm period of the year (April, May, June, July and August). We were therefore interested in choosing opaque and thermally insulated surfaces for these walls (north wall and roof) in order to reduce overheating of the greenhouse during the summer and thermal losses during the winter.

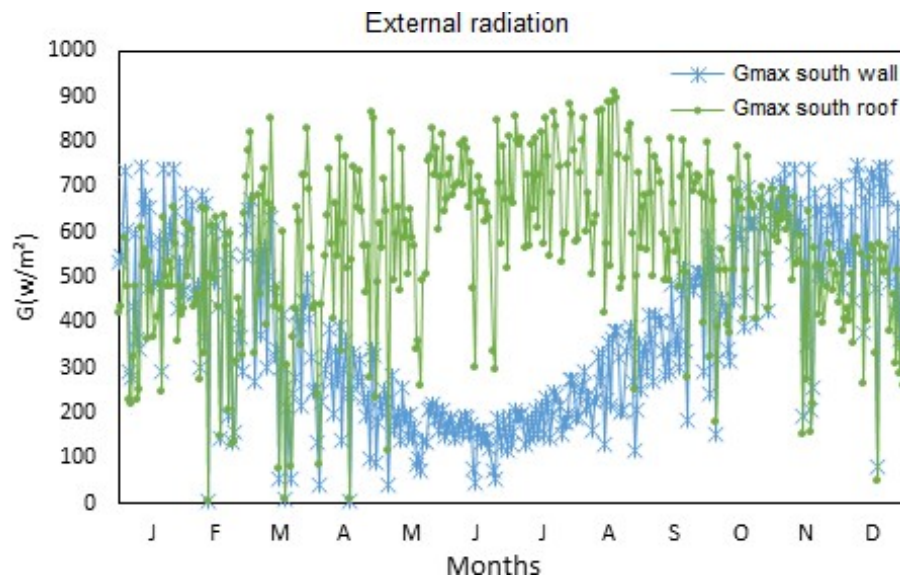


Fig 6: Curves of direct solar radiation (daytime maximums) reaching the main surfaces of the greenhouse (south wall, south roof) depending on the months of the year.

Figure 7 shows the temperature variation curves (daytime maximums and nighttime minimums respectively) of the different components of the greenhouse, depending on the months of the year.

During the day, the temperature of the plant cover is the highest; it is this which causes the rise in air temperature. It presents notable differences with that of indoor air. The average differences between the maximum daytime temperatures of the plant cover and those of the indoor air vary from 7°C (cold period of the year) to 10°C (hot period of the year).

At night, the ground surface temperature is highest; the temperature of the plant cover and that of the indoor air evolve in the same way.

Incident solar radiation gradually decreased from 1.5 m to 0 m, suggesting that lower solar radiation was obtained when closer to the floor and vice versa, because lush foliage blocks the ground to receive more sunlight (li and Zhang, 2017).

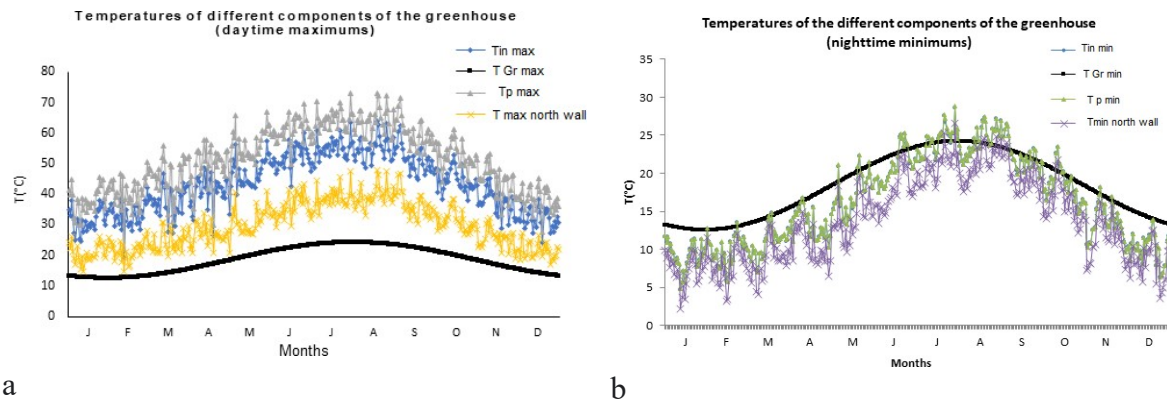


Fig 7: Daytime maximum (a) and nighttime minimum (b) temperature variation curves of the different components of the greenhouse, depending on the months of the year.

2. Plant evapotranspiration:

According to Baglivo et al. (2020) in the study considering the growth of the chrysanthemum, the evapotranspiration produced by the plant influences the simulation.

Figure 8 shows the variation curve of the mass flux densities exchanged by evapotranspiration as a function of time. We see that this curve takes the same shape as that of sunshine. The peaks of this curve (daily maximums) vary depending on the greenhouse climate. Strangellini, 1995 experimentally determined evapotranspiration in greenhouses. He found a similar curve (of the same shape) with peaks of around $80\ (\text{mg}/\text{m}^2\text{s})$.

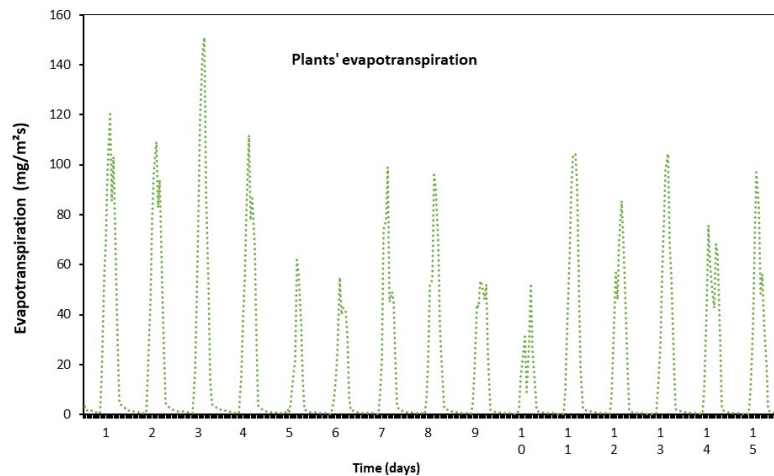


Fig 8: Curves of variation of mass flux densities exchanged by evapotranspiration as a function of time (January 1-15)

Figure 9a shows the maximum daily evapotranspiration as a function of the days of the year. We note that the evapotranspiration of plants during the months May, June, July, August, September is much higher than that during the rest of the year ($895\text{mg}/\text{m}^2\text{s}$). This can be explained by the fact that the temperature during these months (May, June, July, August, September) is very high, so the plant's water needs will increase exponentially. This can cause water stress for the plant.

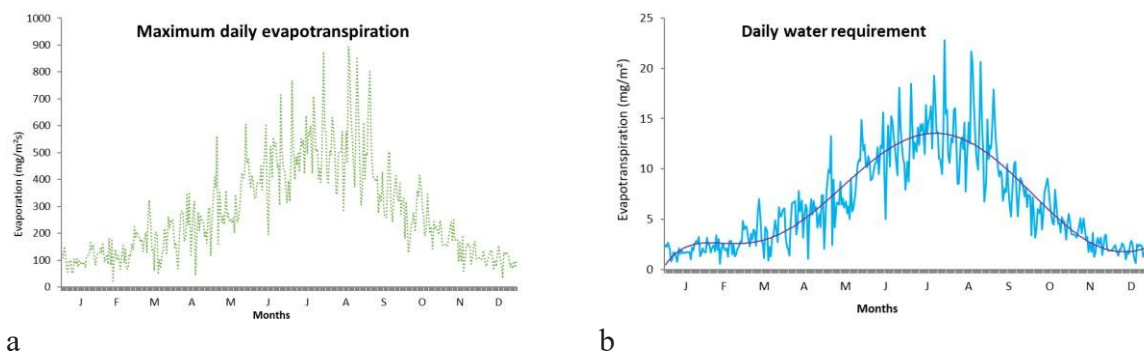


Fig 9: Maximum daily evapotranspiration curve (a) and the daily water requirements of the crop (tomato), compared to the unit surface area of the leaves (b).

Katsoulas (2002) indicates that reducing incoming solar radiation in the greenhouse resulted in a canopy vapour air pressure deficit. He also notes that during the period without shading, the canopy air vapour pressure deficit was high; however, shading the greenhouse led to the crop experiencing no heat or water stress. Consequently, the same author mentions that shading the greenhouse resulted in lower crop temperatures and increased crop stomatal conductance and transpiration rate. Finally, several researchers stipulate that greenhouse shading is a source of a decrease in temperature and transpiration rate (Boulard et al., 1991; Abreu and Meneses 2000; Dayan et al., 2000; Fernandez-Rodriguez et al., 2000) and crop production (Sellami et al., 2018).

In the figure 9b the daily water requirements of the crop (tomato) are represented, compared to the unit surface area of leaves. This curve has the same shape as the previous one. The thermal environment of the plant (infrared radiation) has a significant effect on its water consumption.

3. Influence of leaf area index

a. Air temperature

Figure 10 represents the variation curves of indoor air temperature (daytime maximums and nighttime minimums) for a bare greenhouse without vegetation (LAI=0) and a greenhouse cultivated with different leaf indices (LAI=2, 4 and 6) depending on the months of the year.

During the day, the air temperature in the greenhouse increases with the leaf area index. The more developed the culture (LAI is larger), the higher the indoor air temperature. The plant, in the greenhouse, plays the role of a heat absorber. In fact, the plant absorbs solar energy and diffuses the absorbed heat through infrared radiation and convection. This has the effect of increasing the air temperature. The more external cells of the leaf will transmit the excess kinetic energy to the ambient air. This effect reduces its temperature and increases that of the air. Subsequently, the boundary layer which accumulates this energy can increase or decrease the energy transfer depending on its resistance (Erik Runkle, 2016). High resistance decreases heat transfer because the energy flow of the masses keeps the heat of the leaf around it when there is little air change in the boundary layer and the foliage is of large area. Low resistance, on the contrary, increases heat transfer. The energy flow of the masses involved will be lower due to the large air changes of the boundary layer and the small surface area of the leaves.

The process of energy transfer and temperature regulation in plant leaves involves the mesophyll cells, which play a crucial role in photosynthesis and managing heat within the leaf. The palisade parenchyma and spongy parenchyma within the leaf structure facilitate the

exchange of gases and help in dissipating excess heat to the surrounding environment (Vogelmann and Martin, 2006).

The increase of the inside leaf temperature activates the transpiration mechanism. The release of water from the leaf surface causes the phenomenon of evaporation which transfers energy from the liquid medium to a gaseous medium with the aim of reducing the internal temperature of the leaf.

Plant transpiration increases with temperature. Above 30°C, the stomata close and photosynthesis decreases. From 45°C, it is completely inhibited. Gounaris et al. (1983) showed that above 50°C, there is a disruption in the protein-lipid interactions of membranes. Thermal stress first damages membranes, then tissues, and induces cell contraction/expansion.

In response to high temperature, some plants, such as peas, increase the lipid concentration of the membrane, and can then continue to photosynthesize.

At night, the indoor air temperature variation curves, for different leaf indices, are combined. The presence of greenhouse cultivation has no effect on air temperature.

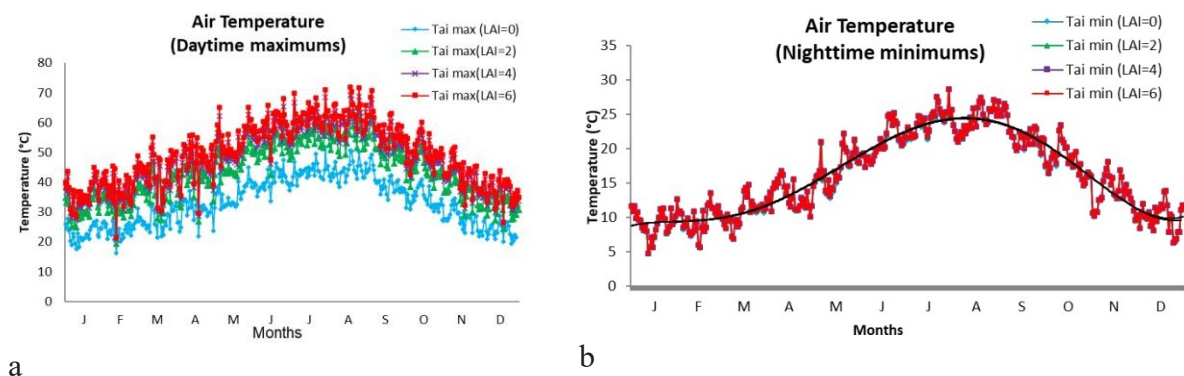


Fig10: Indoor air temperature variation curves (daytime maximum) (a) and nighttime minimum (b) for an uncultivated greenhouse (LAI=0) and a cultivated greenhouse (LAI=2, 4 and 6) as a function of the months of the year.

b. Relative humidity

Figure 11 represents the relative humidity variation curves (nocturnal maximums and daytime minimums) for different leaf indices (LAI=0, 2, 4 and 6) as a function of the months of the year. At night, the variation curves of the relative humidity of the indoor air, for LAI=2, 4 and 6, are combined. The relative humidity of a greenhouse without vegetation (LAI=0) is slightly higher than that of a cultivated greenhouse. The average differences between the relative humidity of a bare greenhouse and a cultivated greenhouse vary from 3% (cold time of year) to 8% (hot time of year). Plant size (leaf area) has no effect on relative air humidity.

During the day, the relative humidity of the air in the greenhouse decreases with the leaf area index. The more developed the canopy (larger LAI), the lower the relative humidity. This is essentially due to the increase in indoor air temperature depending on the leaf area index which determines a decrease in relative humidity.

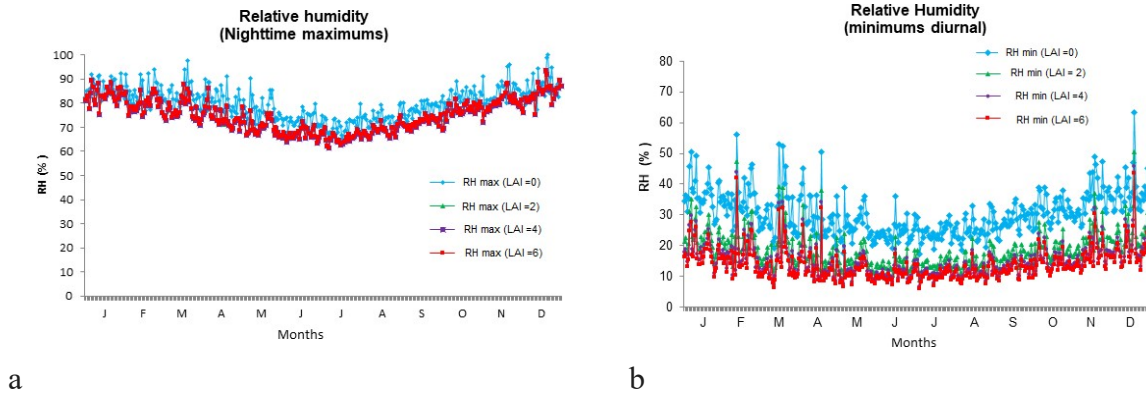


Fig 11: maximum nighttime (a) and minimum daytime (b) relative humidity variation curves (for an uncultivated greenhouse (LAI=0) and a cultivated greenhouse (LAI=2, 4 and 6) as a function of the months of the year.

c. Plant temperature

In figure 12, the variation curves of the plant temperature (daytime maximums and nighttime minimums respectively) are represented for different leaf indices (LAI=2, 4 and 6) as a function of the months of the year. We see that the temperature fluctuations of the plant exhibit the same behavior as that of the air temperature. Indeed, during the day, the plant temperature increases with the leaf area index. The more the plant cover is developed (LAI is greater), the higher the plant temperature. At night, the plant cover temperature curves are confused with that of the indoor air. The effect of the presence of culture is negligible. There is no difference between the nighttime temperatures of a well-grown or less-grown crop and the air inside the glass greenhouse. Also, there is no difference between the temperature of a cultivated greenhouse and a greenhouse without vegetation.

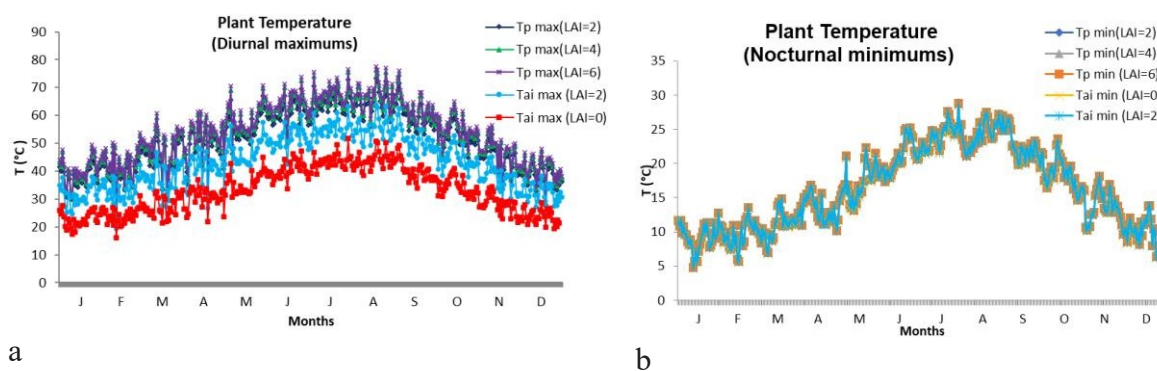


Fig 12: Air and plant (Tomato) temperature variation curves (diurnal maximums) (a) and (nighttime minimums) (b) for different leaf indices (LAI=0, 2, 4 and 6) depending on the months of the year.

d. Water requirements of plants

In the figure 13, the monthly water requirements of the crop (tomato) are represented, related to the leaf surface unit, for different leaf indices (LAI=2, 4 and 6), depending on the months of the year. We see that the water needs of plants during the months of May, June, July, August and September are much higher than those during the other months (cold period of the year). There is no notable difference between the water requirements of plants relative to the unit surface area of leaves for different leaf indexes (LAI=2, 4 and 6). The slight difference existing is mainly due to the slight difference existing in the temperature of the air and the plant.

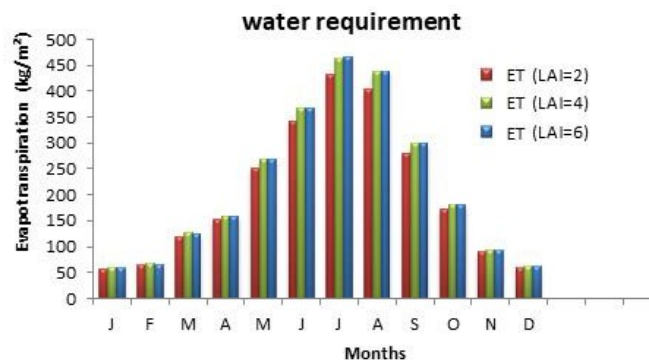


Fig 13: The monthly water requirements of the crop (tomato), related to the unit surface area of leaves, for different leaf area indices (LAI=2, 4 and 6), depending on the months of the year.

As the greenhouse design parameters gradually improved, vegetables were produced in the greenhouse without additional heating during the winter, with temperature differences of 21 °C–25 °C between the inside and outside in areas from 32°N to 41°N in Tunisia.

In order to provide the best indoor air quality to maximize the plant production with minimum consumption of energy, the desiccant cooling system seems to be the most promising system in hot and humid climate.

e. Heating requirement

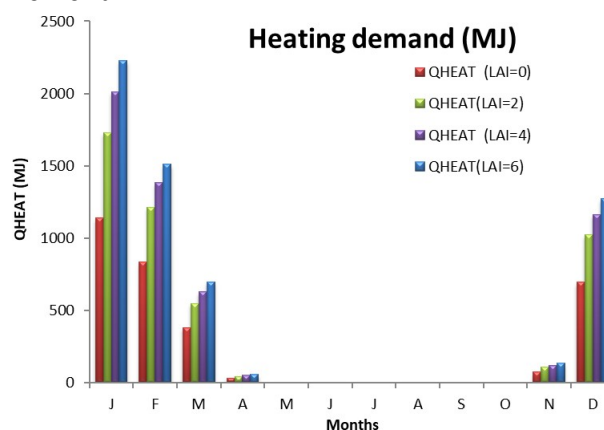


Fig 14: The monthly heating requirements of the crop (tomato), for different leaf indices (LAI=2, 4, 6), depending on the months of the year.

In figure 14, the heating needs of the greenhouse are represented, for different leaf indices (LAI=2, 4 and 6), depending on the months of the year. We note that heating needs increase with leaf area index. The more developed the crop (LAI is larger), the higher the heating

requirements. At night, the plant, in the greenhouse, plays the role of a heat diffuser. In fact, the plant absorbs the energy coming from the heating system and diffuses the absorbed heat by infrared radiation towards the walls of the greenhouse which are made of glass. The more developed the culture (LAI is greater), the more important the exchanges are. This has the effect of increasing heating needs.

4. Improvement of the greenhouse climate

Although the solar greenhouse, studied above, is made of glass, its performance is not satisfactory. In fact, the average differences between nighttime temperatures inside and outside the greenhouse, during the cold period of the year, do not exceed 2°C. During the months of December, January, February and March, night temperatures are lower than the temperature $T_{N\min}=12^{\circ}\text{C}$ required by the plant. The relative humidity of indoor air, during the day, reaches excessively low values (less than 25%). For nine months out of twelve (March to November) daytime temperatures exceed the overheating temperature. Heating the greenhouse during the winter requires a fairly significant amount of energy, around 4600 MJ. In this paragraph we propose to improve the thermo-energetic performance of the greenhouse by thermally insulating, initially, the north wall and the north roof in order to reduce the overheating of the greenhouse during the summer and the thermal losses during the winter. Next, we study the effect of the introduction of heat shields on the microclimate. It is therefore a question of studying two other types of greenhouses: a glass greenhouse of which along the north face (wall and roof) is made up of a sandwich panel wall designated as a "greenhouse with sandwich panels" and a greenhouse with sandwich panels equipped with a thermal screen open from 8 a.m. to 6 p.m. The characteristics of the sandwich panel and the heat shield are presented in the following table (table 2):

Table 2: Characteristics of the sandwich panel wall and the heat shield

Kind	Layers	Thick-ness (m)	Resistance (hm ² K/KJ)	Conductivity (J/hmK)	Capacity (KJ/KgK)	Density (Kg/m3)
Sandwich panel	Galvanized sheet	0.007	1.21	52	0.1	0.1
	Poly-Exp	0.040		0.141	1.38	25
	Polyurethane	0.100		0.108	0.837	35
Thermal screen	Insulation (Low density polyurethane)	0.05	0.625	0.08	1.47	35

Figure 15 represents the indoor air temperature variation curves (maximum daytime and minimum nighttime respectively) for a glass greenhouse, a greenhouse with sandwich panels and a greenhouse with panels sandwiches equipped with a heat shield depending on the months of the year. We observe that:

- At night, the air temperature in a greenhouse with sandwich panels is slightly higher than that in a glass greenhouse. The average differences between air temperatures in a sandwich panel greenhouse and in a glass greenhouse do not exceed 1°C. The thermal insulation of the

greenhouse by the north wall and the north roof only saved 1°C. On the other hand, there are notable differences between the air temperature in a greenhouse with sandwich panels equipped with a thermal screen and that in a greenhouse with sandwich panels. The average differences between the air temperatures in a greenhouse with sandwich panels equipped with a thermal screen and that in a greenhouse with sandwich panels vary from 6 °C (cold period of the year) to 10 °C (hot period of the year). The contribution of thermal screens to reducing heat losses is very satisfactory.

- During the day, there are notable differences between the air temperature in a greenhouse with sandwich panels and that in a glass greenhouse. The average differences between air temperatures in a sandwich panel greenhouse and in a glass greenhouse vary from 4 to 6°C. We also note that the presence of the thermal screen has no notable effect on the daytime air temperature.

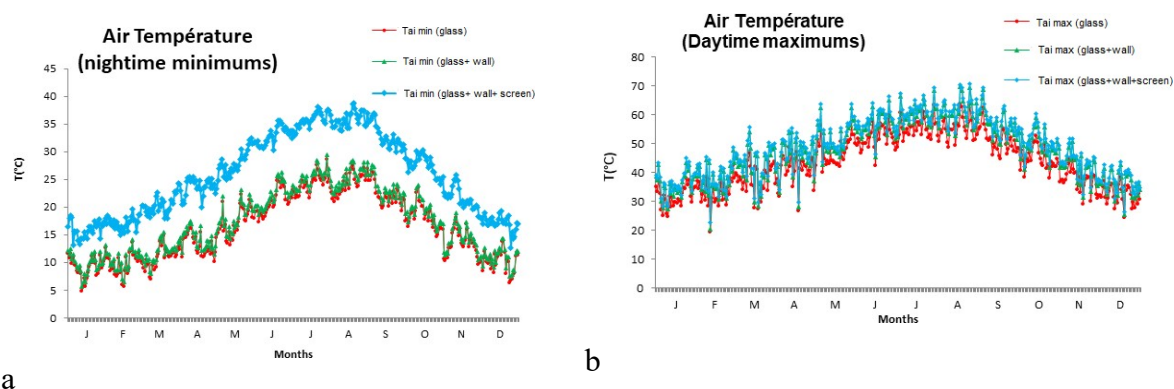


Fig 15: Indoor air temperature variation curves (nighttime minimums) (a) and (daytime maximums) (b) for a glass greenhouse, a greenhouse with sandwich panels and a greenhouse with sandwich panels equipped with a thermal screen depending on the months of the year.

Figure 16 represents the relative humidity variation curves (maximum nighttime (a) and respectively minimum daytime (b)) for a glass greenhouse, a greenhouse with sandwich panels and a greenhouse with sandwich panels equipped with a thermal screen depending on the months of the year, we notice that:

- At night, the relative humidity of the indoor air for a greenhouse with sandwich panels is slightly lower than that in a glass greenhouse. The average differences between air humidity in a sandwich panel greenhouse and in a glass greenhouse vary from 4 to 6%. On the other hand, there are notable differences between the relative humidity of the air in a greenhouse with sandwich panels equipped with a thermal screen and that in a greenhouse with sandwich panels. The average differences between air humidity in a greenhouse with sandwich panels and in a greenhouse with sandwich panels equipped with a thermal screen vary from 25% (cold period of the year) to 30% (hot period of the year). The contribution of thermal screens to reducing relative humidity is very important.
- During the day, there is no remarkable difference in the variation of relative air humidity within the three types of greenhouses.

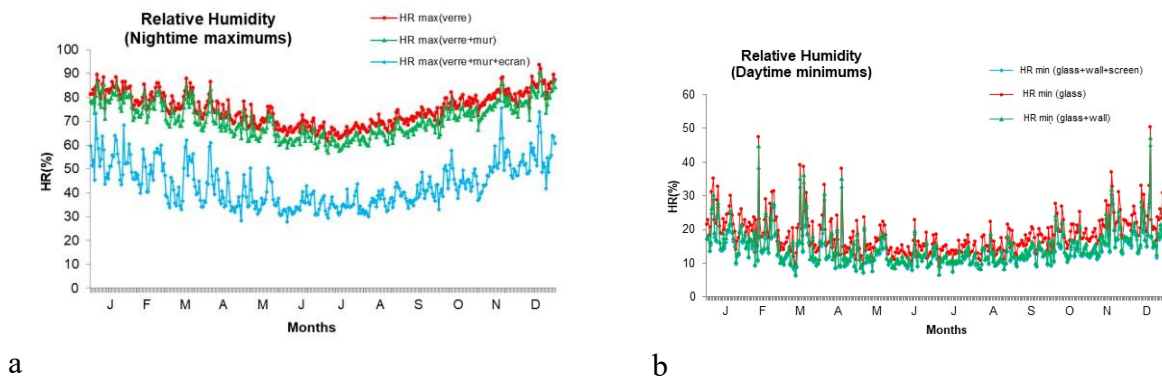


Fig 16: Maximum nighttime (a) and minimum daytime (b) relative humidity variation curves for a glass greenhouse, a greenhouse with sandwich panels and a greenhouse with sandwich panels equipped with a thermal screen depending on the months of the year.

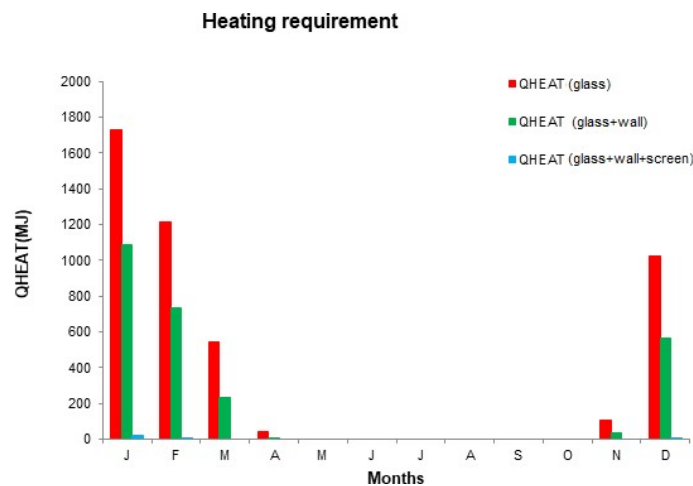


Fig 17: Heating requirements of the crop (tomato), for a glass greenhouse, a greenhouse with sandwich panels and a greenhouse with sandwich panels equipped with a thermal screen depending on the months of the year.

Figure 17 shows the greenhouse heating requirements for a glass greenhouse, a greenhouse with sandwich panels and a greenhouse with sandwich panels equipped with a thermal screen, depending on the months of the year.

We observe that:

During the night period, heating needs are high in a glass greenhouse (1728 MJ, during the month of January). We also note that the presence of a thermal screen reduces the heating requirement to zero (0 MJ).

For the design, analysis and control of the greenhouse system, dynamic simulation, based on knowledge of the system, is crucial. Dynamic modeling of greenhouses is a complex operation that requires long-term work. Given their interest, numerous dynamic models have been developed (Kimball, 1973; Kindelan, 1980; Chandra et al., 1981; Van Bavel et al., 1981; Bot, 1983; Arinze et al., 1984; Monteil, 1985; Deltour, 1985; Kimball, 1986) Each of these models provides improvements compared to the previous ones in terms of: quantification of the light transmission of the cover (Bot, 1983; Critten, 1993), ventilation (De Jong, 1990; Boulard and

others, 1996), plant transpiration (Stanghellini, 1987), energy supply (De Zwart, 1996) and heat shields (Bakker and Van Holsteijn, 1995; Miguel et al., 1998). Other improvements have been made to:

- Precision: this was achieved by a more precise determination of the exchange coefficients, by improving the structure of the model and by a reduction in the number of hypotheses previously taken.
- The diversification of applications of the model and its use as a guide for experiments and control.

Dynamic modeling is a proven tool in greenhouse analysis (De Zwart and Bot, 1997). In greenhouse control, models can be reduced to the kernel to describe the dynamics of control variables (Van Straten, 1999) and they can extend from black box to mechanistic models.

However, dynamic models also face the following problems:

- They often require calibration on experimental results (Cormary et al., 1985); which makes the model of limited flexibility and of use reserved only for research. The need for calibration comes either from a bad mathematical description of the phenomena, or from a bad evaluation of certain parameters.
- They are not general and flexible enough to apply to different types of greenhouses. In particular, when it comes to studying the applicability of energy storage (transition from a light wall to a mass wall). The combination with dehumidification and heat pump coupling complicates the model.
- They cannot guide the evolution of the greenhouse climate through regulatory laws. The application for the control is remote due to the complexity and long calculations of this type of modeling.
- Dynamic modeling of greenhouses is not a standard operation. Indeed, the quantification of the various energies and mass transfer processes in greenhouses and the methods for solving the balance equations differ from one model to another.

These different arguments as well as the diversity of applications in greenhouses (cited above) made us think of looking for a dynamic simulation platform on which the modeling of greenhouses will be a standardized operation which reduces modeling constraints.

5. Outcomes

In Tunisia, the sustainable availability of this renewable resource highly encouraged its use in agriculture. In this context, we studied the efficiency of the solar energy for tomato production under greenhouse.

In the greenhouse equipped with a thermal screen, fruit maturity was held to early in 08 April. Compared with plants grown under the greenhouse with sandwich panel, the maturity of fruits of plants grown under glass greenhouse was later by two weeks which took place by 22 April. The difference between the greenhouses concerning the cumulated fruit yield was conspicuous (Table 3). In the greenhouse equipped with a thermal screen, the total crop harvested was equivalent at average to 96.2 t ha^{-1} (equivalent to $50.9 \text{ kg plant}^{-1}$). The total harvest is formed by a major quantity of marketable fruits and a low quantity of undersized fruit. As to greenhouse with sandwich panel, the harvest was more or less similar to that of the glass greenhouse with 84 t ha^{-1} and 67 t ha^{-1} , respectively. But, the majority harvest of greenhouse with sandwich panel consists of undersized fruit with 32 t ha^{-1} against 39 t ha^{-1} in the glass one.

Table 3: Total weight, marketable fruits and undersized fruits of tomato fruits (kg plant^{-1} and equivalent in t ha^{-1}) grown for 20 weeks in greenhouses (Glass, Glass+wall and Glass+wall+screen). Means with different letters are significantly different (NMK-test, $p < 0.05$).

Greenhouses	Marketable fruits		Undersized fruits		Total yield	
	kg plant^{-1}	t ha^{-1}	kg plant^{-1}	t ha^{-1}	kg plant^{-1}	t ha^{-1}
Glass	15 c	28 b	21 a	39 a	36 b	67 b
Glass+wall	28 b	52 b	17 b	32 b	45 b	84 b
Glass+wall+screen	49.6 a	93.8 a	13 c	24 c	50.9a	96.2 a



Fig 18. The outcomes of the monitoring and control of the greenhouse climate conditions for tomato crops under the greenhouse equipped with a thermal screen.

IV. Conclusion:

The management of greenhouse condition includes several physiological processes that influence the growth of plants, such as lighting, temperature, humidity, soil nutrient and soil temperature.

The simulations obtained for the solar greenhouse studied were carried out for the climate of Tunis, over the whole year. The numerical simulation results show that the thermal performance of the solar greenhouse, despite being constructed of glass, is not satisfactory. In fact, the average differences between nighttime temperatures inside and outside the greenhouse, during the cold period of the year, do not exceed 2°C . During the months of December, January, February and March, night temperatures are lower than the minimum temperature required by the plant ($T_{Nmin}=12^{\circ}\text{C}$). The relative humidity of indoor air, during the day, reaches excessively low values (less than 25%). For nine months out of twelve (from March to November) daytime temperatures exceed the overheating temperature ($\text{Overheating}=32^{\circ}\text{C}$). Heating the greenhouse, with an area of 100 m^2 , during the winter requires a fairly significant amount of energy of around 4600 MJ.

We proposed to improve the thermo-energetic performance of the greenhouse by thermally insulating, initially, the north wall and the north roof in order to reduce overheating of the greenhouse during the summer and thermal losses during the winter. , and subsequently, by introducing thermal screens in the greenhouse.

We found that, at night, the air temperature in a greenhouse with sandwich panels is slightly higher than that in a glass greenhouse. Thermal insulation of the greenhouse by the north wall and the north roof only saved 1°C. On the other hand, we recorded notable differences between the air temperature in a greenhouse with sandwich panels equipped with a thermal screen and that in a greenhouse with sandwich panels. The average differences between the air temperatures in a greenhouse with sandwich panels equipped with a thermal screen and that in a greenhouse with sandwich panels, during the cold period of the year, are of the order of 6°C. The contribution of thermal screens to reducing heat losses is very satisfactory. The contribution of thermal screens to reducing relative humidity during the night is very significant (around 25%). The presence of thermal screens in the greenhouse reduces the heating requirements of the greenhouse to zero (0MJ) (to maintain it at a temperature greater than or equal to $T_{min}=12^{\circ}\text{C}$ during the night).

References

- [1]. A. Deiana, E. Fabrizo, R. Gerboni 2014. Energy performance optimization of typical Chinese solar greenhouses by means of dynamic simulation, in: Interanational Conf. Agric. Eng., Zurich, pp. 6–10.
- [2]. A. Vadiée, V. Martin 2013. Energy analysis and thermoeconomic assessment of the closed greenhouse-The largest commercial solar building. *Appl. Energy*. 102, 1256–1266. doi:10.1016/j.apenergy.2012.06.051.
- [3]. Abreu, P. E., Meneses, J. F., 2000. Influence of soil covering, plastic ageing and roof whitening on climate and tomato crop response in an unheated plastic Mediterranean greenhouse. *Acta Horticulturae*. 534, 343-350.
- [4]. Angui Li, Lin Huang, Tongfeng Zhang, 2017. Field test and analysis of microclimate in naturally ventilated single-sloped greenhouses, *Energy and Buildings*. 138, 479-489. <http://dx.doi.org/10.1016/j.enbuild.2016.12.047>
- [5]. Arinze, E. A. Schoenau, G. J. Besant, R. W. 1984. A dynamic thermal performance simulation model of an energy conserving greenhouse with thermal storage. *Transactions of the American Society of Agricultural Engineers*, 27(2): 508.-5 19.
- [6]. Avik Sinha , Tuhin Sengupta , Olga Kalugina, Muhammad Awais Gulzar, 2020; Does distribution of energy innovation impact distribution of income: a quantile-based SDG modeling approach. *Technol. Forecast. Soc. Change*. 160. <https://doi.org/10.1016/j.techfore.2020.120224>
- [7]. Guo, X.X. Wang, L. Pei, Y. Su, D.M. Zhang, Y. Wang 2020. Identifying the spatiotemporal dynamic of PM2.5 concentrations at multiple scales using geographically and temporally weighted regression model across China during 2015–2018. *Sci. Total Environ.*, 751, Article 141765.

- [8]. Bakker, J.C. Van Holsteijn, G.P.A. 1995. Screens. In: Bakker, J.C., Bot, G.P.A., Challa, H., Van de Braak, N.J. (Eds.), *Greenhouse Climate Control, an Integrated Approach*. Wageningen Press, pp.185–195.
- [9]. Bot, G.P.A. 1983. *Greenhouse climate: from physical processes to a dynamic model*, PhD thesis, Wageningen University, p. 239.
- [10]. Boulard, T. Meeses, J.F. Mermier, M. Papadakis, G. 1996. The mechanisms involved in the natural ventilation of greenhouses. *Agric. For. Meteor.* 79, 61–77.
- [11]. Boulard, T., Baille, A., Le Gall, F., 1991. Etude de différentes méthodes de refroidissement sur le climat et la transpiration de tomates de serre. *Agronomie* 11: 543-554.
- [12]. Chandra, P. Albright L. D. et Scott N. R. 1981. A time dependent analysis of greenhouse thermal environment, *Transaction of ASAE*, 24, 442-449.
- [13]. Chunhong Zhang , Irfan Khan , Vishal Dagar , Asif Saeed , Muhammad Wasif Zafar, 2022. Environmental impact of information and communication technology: Unveiling the role of education in developing countries. *Technological Forecasting and Social Change* 178. <https://doi.org/10.1016/j.techfore.2022.121570>.
- [14]. Cormary, Y. Nicolas, Ch et Brun, R. 1985. *La thermique des serres*. Editions Eyrolles, Paris France, 353 p.
- [15]. Cristina Baglivo, Domenico Mazzeo, Simone Panico, Sara Bonuso, Nicoletta Matera, Paolo Maria Congedo, Giuseppe Oliveti, 2020. Data from a dynamic simulation in a free-floating and continuous regime of a solar greenhouse modelled in TRNSYS 17 considering simultaneously different thermal phenomena. *Data in Brief*, 33, 2352-3409.
- [16]. Critten, D.L. 1993. A review of the light transmissivity into glasshouse crops. *Acta Hort.* 328, 9–31.
- [17]. Dayan, E., Fuchs, M., Plaut, Z., Presnov, E., Grava, A., Matan, E., Solphoy, A., Mugira, U., Pines, N., 2000. Cooling of roses in greenhouses. *Acta Horticulturae*, 534: 351-360.
- [18]. De Jong, T. 1990. *Natural ventilation of large multi-span greenhouses*, PhD Thesis, Wageningen University, 116 p.
- [19]. De Zwart, H.F. 1996. *Analysing energy saving options in greenhouse cultivation using a simulation model*, PhD thesis, Wageningen University, p.236.
- [20]. De Zwart, H.F. Bot, and G.P.A. 1997. Energy saving perspectives of combined heat and power generation in The Netherlands: a simulation study. *Neth. J. Agric. Sci.* 45 (1), 97–110.
- [21]. Deltour, J. 1985. Dynamic modeling of heat and mass transfer in green house. *Acta Horticultural*, 174:119-126.
- [22]. Douja Sellami, Hassen Boughanmi, Salwa Bouadila, Asma Bensalem-Fnayou. 2018. Comparative study of the performance of two greenhouse heating ways: Solar air heater and a heat pump. *Heat Transfer Research* 50(12). DOI: 10.1615/HeatTransRes.2018026690
- [23]. ERIK RUNKLE 2016. Red Light and Plant Growth AUGUST 2016 GPNMAG.COM.

- [24]. Fernandez-Rodriguez, E. J., Fernandez-Vadillos, J., Camacho-Ferre, F., Vazquez, J. J., Kenig, A., 2000. Radiative field uniformity under shading screens under greenhouse versus whitewash in Spain. *Acta Horticulturae*, 534, 125-130.
- [25]. G.G. Das, 2014. Land-use, Land-cover and Food-Energy-Environment Trade-off: Key Issues and Insights for Development Goals, In book: *Encyclopedia of Agriculture and Food Systems*, Elsevier, pp. 114-133. DOI: 10.1016/B978-0-444-52512-3.00081-4
- [26]. GN Tiwari 1984. Analysis of winter greenhouse. *International Journal of Solar Energy*, 3(1):19-24.
- [27]. Guohong Tong; David M. Christopher ; Tianlai Li ; Tieliang Wang ; 2013. Passive solar energy utilization: A review of cross-section building parameter selection for Chinese solar greenhouses. *Renewable and Sustainable Energy Reviews* 26, 540–548.
- [28]. H. Yu, Y. Chen, S.G. Hassan, D. Li 2016. Prediction of the temperature in a Chinese solar greenhouse based on LSSVM optimized by improved PSO, *Comput. Electron. Agric.* 122, 94–102. doi:10.1016/j.compag.2016.01.019.
- [29]. I. Attar, N. Naili, N. Khalifa, M. Hazami, A. Farhat 2013. Parametric and numerical study of a solar system for heating a greenhouse equipped with a buried exchanger, *Energy Convers. Manag.* 70 163–173. doi:10.1016/j.enconman.2013.02.017.
- [30]. Irfan Khan , Abdulrasheed Zakari , Vishal Dagar , Sanjeet Singh 2022 World energy trilemma and transformative energy developments as determinants of economic growth amid environmental sustainability. *Energy Econ.* 108.
- [31]. J. Mao, J. Xie, Z. Hu, L. Deng, H. Wu, Y. Hao 2023. Sustainable Development through Green Innovation and Resource Allocation in Cities: Evidence from Machine Learning, *Sustainable Development*. <https://doi.org/10.1002/sd.2516>.
- [32]. Jin-Li Hu, Shih-Chuan Wang 2006. Total-factor energy efficiency of regions in China, *Energy Pol.* 34 (17), 3206–3217. <https://doi.org/10.1016/j.enpol.2005.06.015>.
- [33]. Kasuda, T. and Archenbach, P.R. 1965. Earth Temperature and Thermal Diffusivity at Selected Stations in the United States. *ASHRAE Transactions*, Vol. 71, Part 1.
- [34]. Kimball, B. A. 1973. Simulation of the energy balance of a greenhouse. *Agricultural Meteorology*, 1 I(2): 243-260.
- [35]. Kimball, B.A. 1986. A modular energy balance program including subroutines for greenhouses and other latent devices. *Agricultural Research Service*.
- [36]. Kindelan, M. 1980. Dynamic modeling of greenhouse environment, *Transaction of ASAE*, 23(5), 1232-1239.
- [37]. Kleoniki Gounaris, David Whitford, James Barber 1983. The effect of thylakoid lipids on an oxygen-evolving Photosystem II preparation. *FEBS Letters*. 163 (2), 230-234.

- [38]. L. Semple, R. Carriveau, D.S.K. Ting 2016. Potential for large-scale solar collector system to 564 offset carbon-based heating in the Ontario greenhouse sector, *Int. J. Sustain. Energy*. 37 565, 378–392. doi:10.1080/14786451.2016.1270946.
- [39]. L. Semple, R. Carriveau, D.S.K. Ting 2017. Assessing heating and cooling demands of closed greenhouse systems in a cold climate, *Int. J. Energy Res.* 41, 1903–1013. doi:10.1002/er.
- [40]. L.B. Liu, Y. Wang, Z. Wang, S.C. Li, G.H. Li, Y. Li, Y.X. Liu, S.L. Piao, Z.Q. Gao, R. Chang, W.J. Tang, K.J. Jiang, S.J. Wang, J. Wang, L. Zhao, Q.C. Chao 2022. Potential contributions of wind and solar power to China's carbon neutrality *Resour Conserv Recycl.*, 180, Article 106115.
- [41]. M.S. Ahamed, H. Guo, K. Tanino 2018. Development of a thermal model for simulation of supplemental heating requirements in Chinese-style solar greenhouses, *Comput. Electron. Agric.* 50, 235–244.
- [42]. Md Shamim Ahamed, Huiqing Guo, Karen Tanino 2020. Modeling heating demands in a Chinese-style solar greenhouse using the transient building energy simulation model TRNSYS. *Journal of Building Engineering.* 29, 101114. <https://doi.org/10.1016/j.jobe.2019.101114>
- [43]. Michael J Savage 2014. Microclimate conditions in ventilated wet-walled greenhouses in a subtropical climate: spatial variability. *South African Journal of Plant and Soil*, 31(3), 137-143.
- [44]. Michael J Savage. 2014. Microclimate conditions in ventilated wet-walled greenhouses in a subtropical climate: spatial variability. *South African Journal of Plant and Soil*, 2014, 31(3):137-143.
- [45]. Miguel, A.F. Braak, N.J. van de, Bot, G.P.A. 1998. Physical modelling of natural ventilation through screens and windows in greenhouses. *J. Agric. Engng. Res.* 70, 165–176.
- [46]. Monteil, C. 1985. Contribution informatique à l'analyse énergétique des serres agricoles. Thèse Doc. Ing, Institut Polytechnique de Toulouse.
- [47]. N. Katsoulas, A. Baille, C. Kittas 2002. Influence of leaf area index on canopy energy partitioning and greenhouse cooling requirements. *Biosyst. Eng.*, 83 (3), 349-359.
- [48]. Nathaniel, S.P. 2020. Ecological footprint, energy use, trade, and urbanization linkage in Indonesia. *Geojournal* 7. <https://doi.org/10.1007/s10708-020-10175-7>.
- [49]. Nikolaos Katsoulas, Constantinos Kittas 2011. Greenhouse Crop Transpiration Modelling. Chapter In book: *Evapotranspiration - From Measurements to Agricultural and Environmental Applications*. DOI: 10.5772/23470
- [50]. P. Henshaw 2016. Modelling changes to an unheated greenhouse in the Canadian subarctic to lengthen the growing season. *Sustain. Energy Technol. Assessments.* 24, 32–38. doi:10.1016/j.seta.2016.12.004.
- [51]. Shengli Yang , Weirong Wang 2022. The Role of Academic Resilience, Motivational Intensity and Their Relationship in EFL Learners' Academic Achievement *Front Psychol CURRICULUM, INSTRUCTION, AND PEDAGOGY* article. doi: 10.3389/fpsyg.2021.823537.
- [52]. Siano P. 2014. Demand response and smart grids—a survey. *Renew Sustain Energy Rev.* 30, 461–78. <http://dx.doi.org/10.1016/j.rser.2013.10.022>.

- [53]. Sinha, A., Shahbaz, M., Balsalobre, D., 2017. Exploring the relationship between energy usage segregation and environmental degradation in N-11 countries. *J. Clean. Prod.* 168, 1217–1229. <https://doi.org/10.1016/j.jclepro.2017.09.071>.
- [54]. Stanghellini, C. 1987. Transpiration of greenhouse crops. An aid to greenhouse management, PhD Thesis, Wageningen University, 150 p.
- [55]. Stanghellini, C., & de Jong, T. (1995). A model of humidity and its application in a greenhouse. *Agricultural and Forest Meteorology*, 76(2), 129-148. [https://doi.org/10.1016/0168-1923\(95\)02220-R](https://doi.org/10.1016/0168-1923(95)02220-R)
- [56]. Sunil Luthra, Anil Kumar, Manu Sharma, Jose Arturo Garza-Reyes, Vikas Kumar. 2022. An analysis of operational behavioural factors and circular economy practices in SMEs: An emerging economy perspective. *Journal of Business Research*. 141, 321-336. <https://doi.org/10.1016/j.jbusres.2021.12.014>
- [57]. T. Ha, I.-B. Lee, K.-S. Kwon, S.-W. Hong 2015. Computation and field experiment validation of greenhouse energy load using building energy simulation model, *Int. J. Agric. Biol. Eng.* 8, 116–127. doi:10.3965/j.ijabe.20150806.2037.
- [58]. T. Yohannes, H.E. Fath, 2013. Novel agriculture greenhouse that grows its water and power: thermal analysis. *Proceedings of the 24th Canadian Congress of Applied Mechanics (CANCAM 2013)*, Saskatoon, Saskatchewan, Canada.
- [59]. Thomas C. Vogelmann, G. Martin, 2006. The functional significance of palisade tissue: penetration of directional versus diffuse light. *Plant Cell and Environment*. 16 (1) :65–72. DOI: 10.1111/j.1365-3040.1993.tb00845.x
- [60]. Van Bavel, C. H. M. Damagnez, J. et Sadler, E. J. 1981. The fluid roof solar greenhouse: energy budget analysis by simulation, *Agric. Meteor.*, 23, 61-76.
- [61]. Van Straten, G. 1999. Acceptance of optimal operation and control methods for greenhouse cultivation. *Ann. Rev. Control* 23, 83–90.
- [62]. X. Pan, T. Shao, X. Zheng, Y. Zhang, X. Ma, Q. Zhang 2023. Energy and sustainable development nexus: a review, *Energy Strategy Rev.* 47, 635–650. 101078. Policy 86.
- [63]. Zafar, M.W., Zaidi, S.A.H., Khan, N.R., Mirza, F.M., Hou, F., Kirmani, S.A.A., 2019. The impact of natural resources, human capital, and foreign direct investment on the ecological footprint: the case of the United States. *Res. Pol.* 63, 101428 <https://doi.org/10.1016/j.resourpol.2019.101428>.